

# MODIFICATIONS OF THE TIP VORTEX STRUCTURE FROM A HOVERING ROTOR USING SPOILERS<sup>1</sup>

JUSTIN W. RUSSELL AND LAKSHMI N. SANKAR  
*School of Aerospace Engineering*  
*Georgia Institute of Technology, Atlanta, GA 30332-0150*

CHEE TUNG  
*Army Aeroflightdynamics Directorate*  
*NASA Ames Research Center, Moffett Field, CA 94035*

## Abstract

Numerical studies of the tip vortex structure from a hovering rotor with and without various spoilers are presented. A general multizone unsteady three-dimensional Navier-Stokes solver is developed to determine the flowfield. A scheme that is fifth-order accurate in space and first-order accurate in time is used to improve the capturing of the tip vortex. Velocity data from the core of the vortex is studied at various planes behind the blade trailing edge. Computations of this velocity data for a clean rotor are first compared with experimental results obtained for the same rotor test case. Three different trailing edge spoiler configurations are then investigated to see if the tip vortex structure can be favorably altered.

## 1. Introduction

With greater emphasis today being placed on noise reduction both for civil and military rotorcraft, studies of the tip vortices produced by rotors become more and more important. This is because a substantial component of the noise generated by a rotor is due to Blade-Vortex Interaction (BVI), which is the effect of the tip vortex created by previously passing blades on a given blade. Preliminary numerical studies [Lee and Smith] have shown that vortices with larger core sizes have a less detrimental effect on the lift of a blade during BVI. Hence, if the tip vortex can be somehow altered so that

---

<sup>1</sup> Invited Paper, IUTAM Symposium on Dynamics of Slender Vortices, Aachen, Germany, August 31-September 3, 1997.

its core size is substantially increased, then both the BVI noise and the vibratory airloads can be reduced.

Early studies [Tangler] aimed at reducing “blade slap” have shown that passive devices such as a stub/subwing mounted at the rotor tip can be used to improve slap signature with no noticeable degradation in performance. Another rotor has also been tested [Berry and Mineck] with a stub/subwing and a winglet, but a higher torque requirement was found for one test case in hover and therefore these concepts were eliminated from further testing. More recently, devices such as a stub/subwing have been shown to diffuse the tip vortex by as much as 47% with a 9% decrease in drag, and the NASA star tip device has been shown to diffuse the tip vortex by 100% with a 67% increase in drag [Smith and Sigl]. All of these results offer motivation that a passive device, if properly designed, can be used produce significant increases in vortex core size (thus reducing BVI), and in some cases with minimal or no loss in rotor performance.

To properly capture the dynamics of the rotor near-wake, especially those in the vortex core, an accurate solution method is needed. This is particularly true for rotor flows, where the structure of the tip vortex greatly influences the loading on the rotor blade and vice-versa. Higher-order spatial accuracy schemes, such as the one used in the present analysis, have been shown to conserve the vortex structure over large distances [Wake and Choi]. This is necessary if the rotor wake is to properly develop and yield accurate performance predictions. Additionally, this higher-order methodology is needed in order to simulate more complex vortical flows that evolve when passive tip devices are added to simple rotor geometries. It is extremely important to accurately model these vortical flows to be sure that it is the tip device that is altering the vortex core and not the numerics of the scheme.

The present work addresses the aspect of tip vortex modeling (i.e., the details of the velocity field within the core), as well as the study of tip vortex alteration by passive devices. A recent survey [Yu] offers insight into the types of tip alterations that have been tested to reduce BVI noise. However, he notes that only acoustic measurements are taken in these experiments with the tip devices. That is, the physics of the flowfield due to these devices is not well understood. In the case of rotors, the problem is made more complex by the fact that the vortex structure significantly influences the blade loading and vice versa. The present calculations for a clean rotor are compared with experiments [McAlister et al.] to show the effectiveness of the numerical scheme in capturing the dynamics and size of the vortex core. With this established, passive tip devices such as spoilers are then investigated to show their benefits and/or detriments to the rotor and their effects on near-wake characteristics.

### 1.1. A MATHEMATICAL CRITERION FOR VORTEX STABILITY

Theoretical analyses [Leibovich and Stewartson, Stewartson and Leibovich] have shown that diffusion of the tip vortex core, in general, tends to destabilize the tip vortex. A thorough investigation into these theoretical studies has been done [Russell et al., AHS

Forum]. For brevity, only the result is given here. It has been shown that a sufficient condition for vortical flow to be unstable is:

$$|V_z| \frac{d\Omega}{dr} \left[ \frac{d\Omega}{dr} \frac{d\Gamma}{dr} + \left( \frac{dV_x}{dr} \right)^2 \right] < 0 \quad (1)$$

where  $|V_z(r)|$  is the azimuthal (normal) velocity component,  $V_x(r)$  is the axial velocity component,  $r$  is the radial distance from the vortex axis,  $\Omega = |V_z(r)|/r$  is the angular velocity, and  $\Gamma = r |V_z(r)|$  is the circulation.

The result of this stability criterion is that if the core of the tip vortex can be diffused (i.e., make  $d|V_z(r)|/dr$  small where  $r$  is small), this results in an unstable vortex. Hence, the goal behind the use of the trailing-edge spoiler is to decrease the slope of the azimuthal (normal) velocity in the vortex core, especially near the center of the vortex. It will be shown that the higher-order numerical scheme used in the present analysis can capture this variation in slope resulting from the addition of three different trailing-edge spoilers.

## 2. Mathematical Formulation

The mathematical and numerical formulation behind the present approach has been extensively documented [Hariharan]. For brevity, only the general characteristics of the formulation are described here.

This numerical scheme solves the three dimensional, unsteady, compressible Navier-Stokes equations. The inviscid and viscous flux terms are computed using a cell-vertex finite volume formulation. The inviscid fluxes at the cell faces are computed using Roe's approximate Riemann solver [Roe]. This solver requires flow information on the left and right sides of a cell face for each coordinate direction. In this work, this information is obtained using a fifth-order essentially-non-oscillatory (ENO) scheme [Chakravarthy, Harten and Chakravarthy].

The solution is advanced in time using an implicit three-factor diagonal alternating-direction-implicit (ADI) scheme [Pulliam and Chaussee]. This makes the procedure first order accurate in time. In addition, implicit fourth-order artificial dissipation using a spectral radius scaling factor is used to improve the temporal stability characteristics of the scheme.

## 3. Numerical Modeling

For all of the simulations described below, the full Navier-Stokes equations are solved in a time-accurate fashion using the algebraic Baldwin-Lomax turbulence model. The

complexity of the configuration requires that the flowfield be divided into zones or blocks, as will be discussed later. Data is passed between zonal interfaces to ensure fifth-order spatial accuracy throughout the interior of the computational domain. Note, however, that the scheme drops to first-order accurate near solid surfaces and farfield boundaries. Only one blade of the multi-bladed rotor is solved in hover, with a periodic boundary condition used at the azimuthal boundaries.

### 3.1. BOUNDARY CONDITIONS

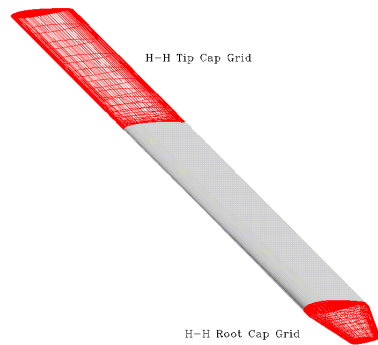


**Figure 1:** Airfoil-Shaped H-H Cap Grids.

All of the farfield boundaries are approximated by a first-order extrapolation. Two-point averages of the flow properties are used at the zonal interfaces. As previously stated, a simple periodic condition is also used at the azimuthal boundaries simulating the existence of other blades. A no-slip boundary condition is used at all solid surfaces. At these surfaces, density is extrapolated to second-order and pressure to first-order. For the blunt ends of the blade, special zones called “cap” grids are used as shown in Figure 1. These cap grids contain singular faces at the leading edge and trailing edge of their airfoil shape.

Here, two-point averages are used just as is done at the leading and trailing edge of the blade surface (due to the H-grid topology).

## 4. Configurations Considered

### 4.1. CLEAN ROTOR

The reference rotor is a model two-bladed rotor which has been experimentally investigated [McAlister et al.]. The grid used for the model consists of 1,210,330 grid points and has an H-H-O topology. The grid is divided into 6 zones with the first two zones forming the H-H-O topology and encompassing a majority of the computational domain. These two zones allow the root and tip airfoil geometries to extend to the farfield boundaries which minimizes grid “kinks” (a source of numerical error) in the radial direction. In most three dimensional simulations for rotors in both hover and forward flight, the grid in the rotor root and tip regions is simply “pinched off”, which physically represents a wedge-shaped end to the rotor root and tip. However, in this simulation we seek to more accurately model the rotor tip geometry and capture the tip vortex. Hence, the rotor root and tip regions are “capped” with two-zone H-H grids that

are in the shape of airfoils of the region from which they extend [see Figure 1]. Note that each zonal interface matches grid point for grid point so as to avoid the use of an interpolation scheme.

#### 4.2. ROTOR WITH TRAILING EDGE SPOILER

In order to make a just comparison between the clean rotor results and the results for the rotor with a spoiler, the exact same grid is used in the spoiler simulations. The only difference between the two grids is that the upper and lower H-H-O zones are split vertically at the trailing edge. This yields a total of 8 zones. A schematic diagram of this configuration is shown in Figure 2 below.

To model the three spoilers, a solid surface boundary condition is applied at the

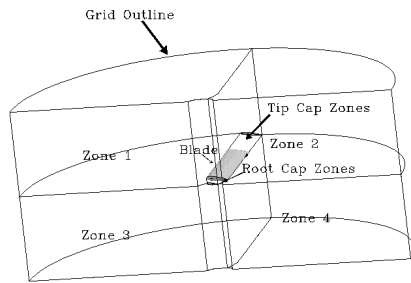


**Figure 2:** Schematic Diagram of Grid Configuration for Simulations of the Rotor with a Trailing-Edge Spoiler.

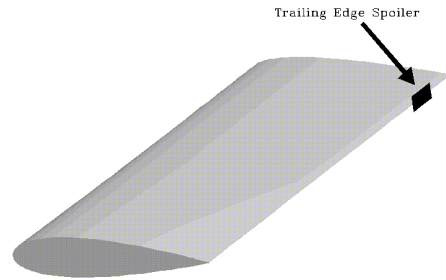


**Figure 3:** Graphical Representation of a Trailing-Edge Spoiler.

trailing-edge zonal interfaces over a range of specified grid points. This yields a spoiler model which is grid-aligned (nearly parallel to the axis of rotation) and of zero thickness. A graphical representation of the trailing-edge spoiler is given in Figure 3 below.

Three different spoiler sizes are tested, with the dimensions and locations as shown below in Table 1.

**Table 1. Dimensions for the Three Spoilers**

Spoiler Number	Height (%chord)	Width (% radius)	Location (% radius)
1	3.9	5.8	87.5 - 93.3
2	5.0	8.8	85.6 - 94.4
3	8.4	13.3	83.5 - 96.8

These dimensions are approximate since the spoiler is actually grid-aligned. The width corresponds to the spanwise dimension and the height is that dimension normal to the flow direction both on the upper and the lower side of the rotor.

## 5. Results and Discussion

### 5.1. CLEAN ROTOR

Results for the clean rotor are first presented to validate the numerical procedure for predicting the characteristics of the vortex core. Results are presented at two instances in time, with the solution starting from a zero-flow initial condition. The measurement plane is the same as that in the experiment. The reader should think of the x-component as the chordwise or axial component (positive towards the blade), the y-component as the radial component (positive inboard), and the z-component as the normal component (positive upward).

Figure 4 below compares the three velocity components in the core of the tip vortex with the experimental data. At this point in time, the blade has traveled only one half of a revolution. The usefulness of this figure is to show that the general characteristics of the tip vortex in the x and z directions can be captured with little computational effort. However, the peak of the y-component (not shown) is not captured at all. This makes sense, since the inboard component is greatly dependent on

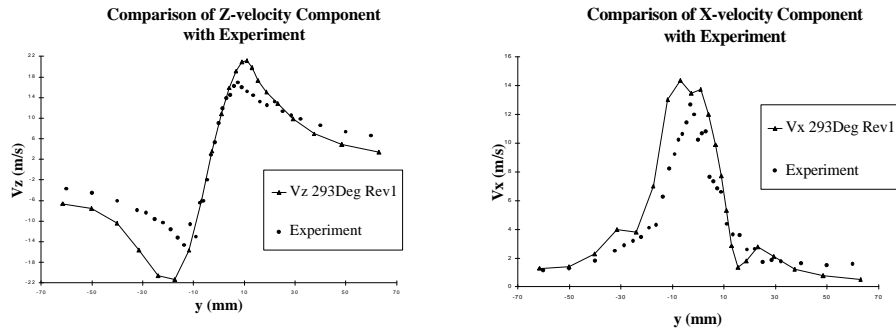


**Figure 4:** Comparison of Core Velocity Component Magnitudes with Experiment for a Clean Rotor; 3 Chordlengths Downstream of the Blade Trailing Edge after One Half of a Revolution.

the wake contraction and the effects of the vortex wake from below. In contrast, the x-component is strongly dependent on the wake viscous effects, and the z-component largely dependent on the lift. Notice that the z-component is overpredicted at the peaks. This is due to the fact that the inflow has yet to develop, which leads to higher lift and consequently higher shed circulation. However, also notice that the thickness of the core and the velocity slope are captured well, which are important for determining stability characteristics.

For visualization purposes, Figure 5 on the following page gives a particle trace in a blade-fixed frame of reference after one half of a revolution. In addition, Figure 6

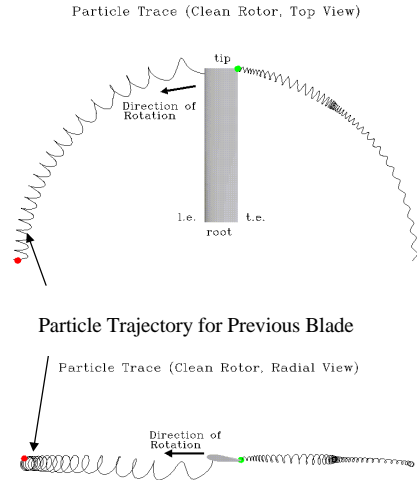


**Figure 5:** Particle Trace (Evolution of the Tip Vortex) after One Half of a Revolution.

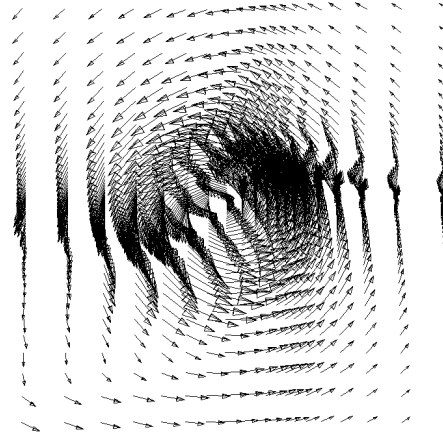


**Figure 6:** Velocity Vectors Showing the Tip Vortex after One Half of a Revolution; 3 Chordlengths Downstream of the Blade Trailing Edge.

(see next page) shows the velocity vectors in the measurement plane. In these figures, the tip vortex has a well-behaved and expected form.

It was expected that simply running the simulation further would improve the results. This was not exactly the case. When beginning from a zero-flow condition, the blade initially sheds a starting tip vortex in the plane of rotation. Hence, once the two-bladed rotor travels one half of a revolution, the second blade hits this starting vortex which causes a large decrease in the lift of the rotor. Consequently, the shed tip vortex becomes weaker, and the predictions worsen. Eventually the inflow reestablishes as the vortices shed by the previous blade are pushed below the blade and the lift recovers. In addition, the wake begins to contract (though rather slowly).

Velocities through the vortex core are presented after one and a half revolutions

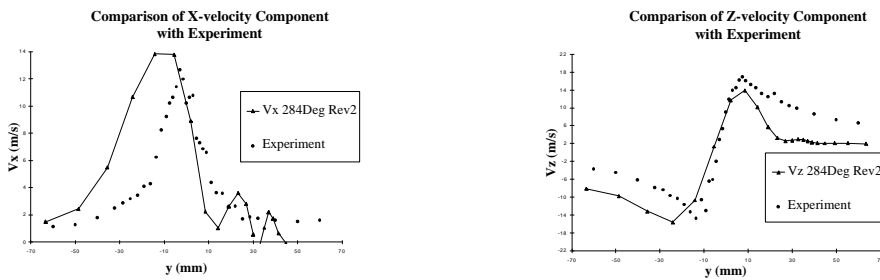
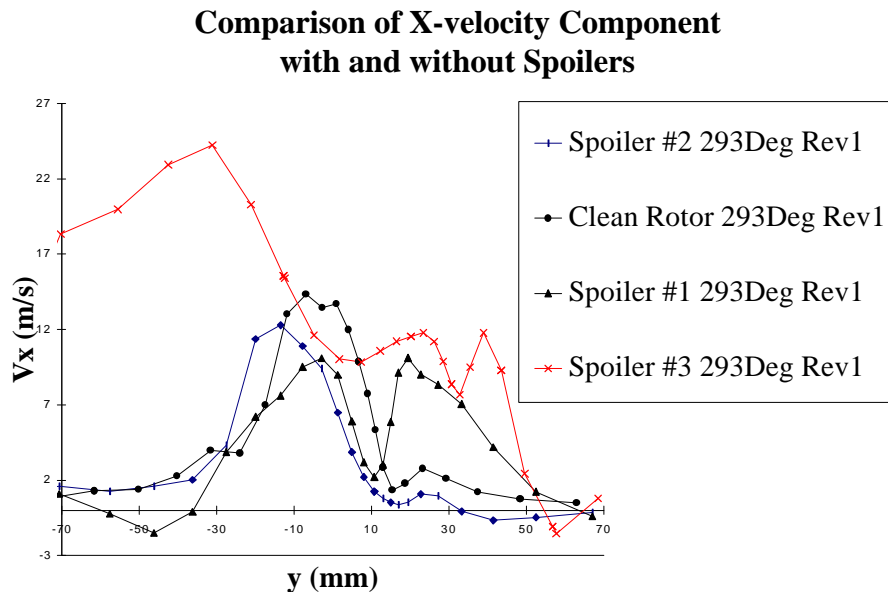


**Figure 7:** Comparison of Core Velocities 3 Chordlengths Downstream of the Blade Trailing Edge after 1.5 Revolutions.

in Figure 7. The magnitude of the peaks for the x and z-components of velocity are predicted well. The y-component (not shown) is still well underpredicted, however some inboard velocity is beginning to form, which is encouraging. Also notice that the vortex thickness is overpredicted. This is due to the fact that the vortex has moved inboard (due to the contraction effects of the vortex below) where fewer grid points exist. This, in effect, “smears” the vortex causing a fatter x-velocity distribution and an underpredicted slope in the z-component velocity distribution. The fact that the axial and normal velocity components are captured well within one half of a rotor revolution, however, allows us to study the destabilizing effects on the tip vortex due to a trailing edge spoiler. Finally, the computed thrust and torque coefficients after one and one half revolutions are  $C_T = 0.0045$  and  $C_Q = 0.00037$  which are lower than McAlister’s values of  $C_T = 0.0051$  and  $C_Q = 0.00052$ . Improvements to these results will be made if the solution is advanced further to a steady-state condition. This is clearly seen in more recent results for a higher tip Mach number case [Russell et al., AIAA Paper 97-1845], where the computed  $C_T$  is 0.00501 compared with a value of 0.00500 from the experiment, and the computed  $C_Q$  value is 0.000531 compared with 0.000500 measured in the experiment.

## 5.2. SPOILER RESULTS

As previously stated, the most important components of velocity through the core of the vortex (as far as stability of the vortex is concerned) are the axial (x) and normal or azimuthal (z) components. Hence, since the goal is to destabilize and diffuse the tip vortex, we will focus only on these components in the vortex core. Figure 8 below and



## Comparison of Z-velocity Component with and without Spoilers

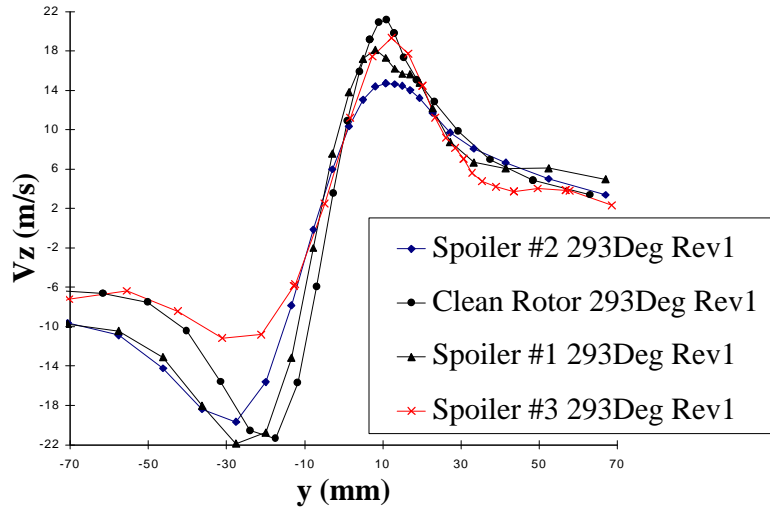


**Figure 8:** Comparison of the Core Velocity Distributions 3 Chordlengths Downstream of the Blade Trailing Edge.

on the next page shows comparisons of the velocity components for the three spoiler configurations with the clean rotor solutions after one half of a revolution.

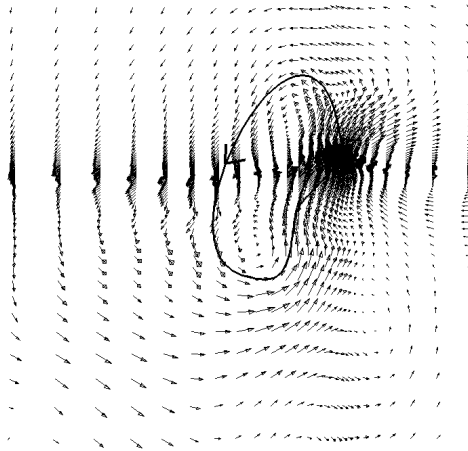
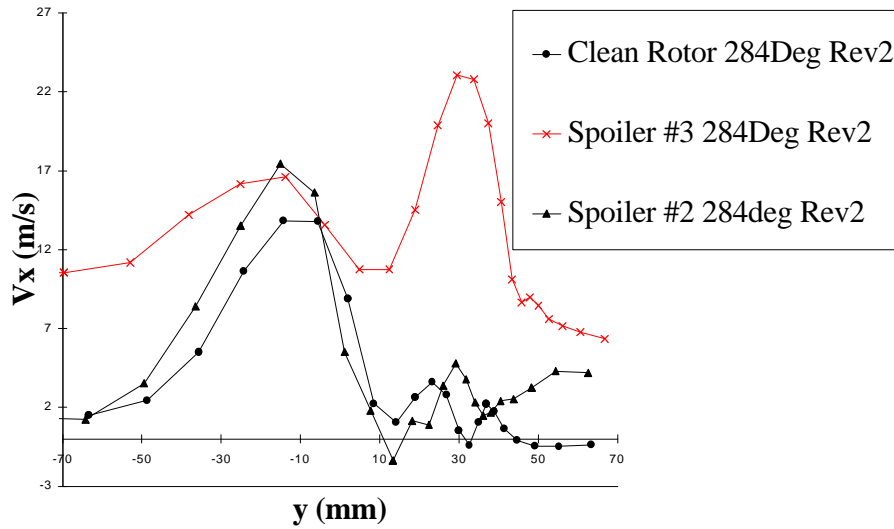


**Figure 9:** Velocity Vectors in the Measurement Plane for the Large Spoiler (#3).

It is evident from the normal velocity distribution that the presence of the spoiler does indeed decrease the slope of the normal velocity distribution in the vortex core. Furthermore, this slope decreases in the core region as the spoiler size increases. Hence, with these results, it is seen that a larger spoiler (as much as excess power would allow) is more beneficial in destabilizing the vortex. Evidence of this destabilization is seen in Figure 9, where the velocity vectors show that the overall organization of the tip vortex degrades downstream for the large spoiler. Again referring to the axial velocity distribution in Figure 8, it is

evident that  $dV_x/dr$  remains relatively large for all spoiler configurations, which is a requirement for vortex destabilization. In addition, the axial velocity distribution for the spoiler cases

### Comparison of X-velocity Component with and without Spoilers



### Comparison of Z-velocity Component with and without Spoilers

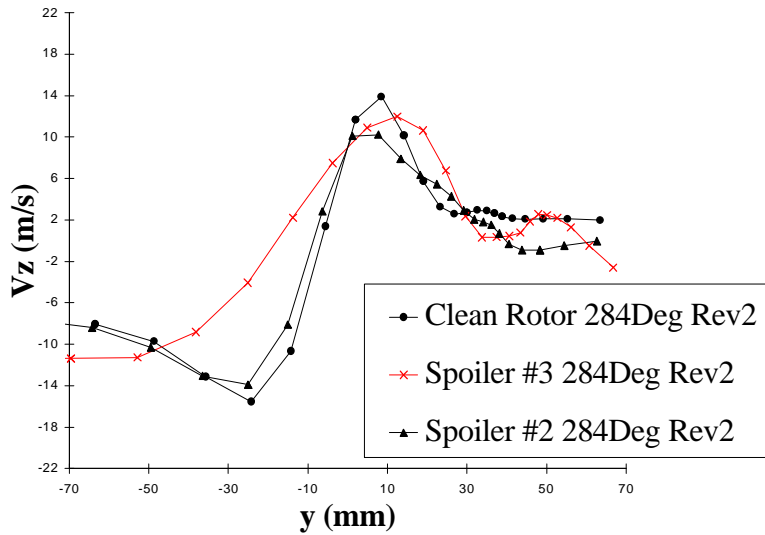


**Figure 10:** Comparison of Velocity Distributions for the Rotor with and without a Trailing-Edge spoilers 3 Chordlengths Downstream of the Blade Trailing Edge after One and a Half Revolutions.

shows that more air is dragged due to the presence of the spoilers, resulting in a significant torque penalty.

The velocity distributions for the rotor/spoiler configurations after one and a half revolutions are shown on the previous page in Figure 10. For comparison purposes, the clean rotor results are also plotted. Notice that the larger the spoiler the less the normal or azimuthal velocity changes in the core, as was seen in the first half revolution. Here, however, the spoiler shows an even more pronounced effect on the slope of the normal velocity through the core. Again, according to equation (1), this has a destabilizing effect on the vortex, which is what we are seeking. Note also that the axial velocity maintains a relatively large slope near the vortex core, with the larger spoiler having a greater “smearing” effect on the distribution.

Overall, the effects of the different spoilers can be seen below in Figure 11 on the following page, which shows the lift coefficient distribution variations for the rotor with the spoilers. Again, the clean rotor results are plotted for comparison. As expected, the presence of the spoiler causes a decrease in lift in the vicinity of its location. Since lift is proportional to the bound circulation on the rotor blade, conservation of vorticity requires that trailing vorticity must be shed due to the radial change in lift. At the inboard station where the lift first drops due to the presence of the spoiler, it is expected that a significant amount of vorticity will be shed forming a vortex that rotates in the same direction as the tip vortex. Also, outboard of the spoiler where the blade experiences a sharp increase in lift, a counter-rotating vortex is expected to be shed. A schematic diagram of this is shown below in Figure 12.

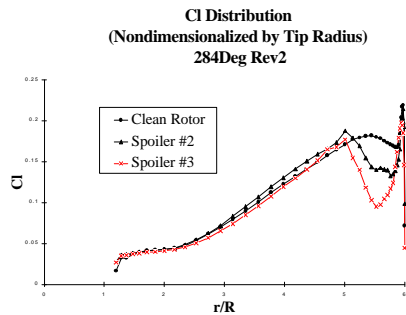


**Figure 11:** Variation in  $C_l$  Distribution for the Rotor Blade with and without Various Spoiler Configurations.

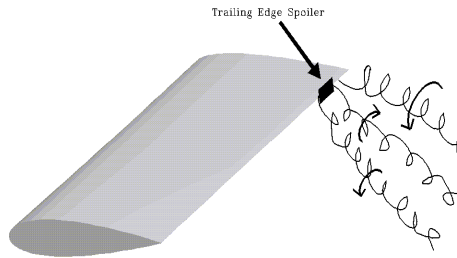


**Figure 12:** Schematic Diagram of Expected Vortex Shedding Due to the Presence of the spoiler.

These effects do indeed occur and can be seen on the following page in Figure 13, which shows the velocity vectors in a radial plane approximately 0.5 chordlengths behind the blade trailing edge. Further downstream, these vortices tend to interact and diffuse the tip vortex to various degrees. The overall effect of this tip vortex alteration is clearly seen in the particle traces shown in Figure 14 on the next page for both spoiler configurations. Comparing these traces with that shown in Figure 5 for the clean rotor,

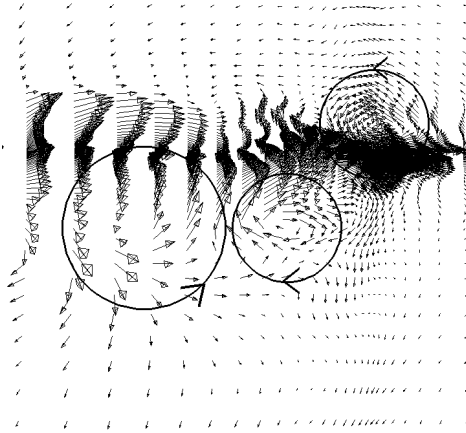


**Figure 13:** Velocity Vectors in the Near Wake of the Rotor with Spoiler #3 Showing Counter and Co-Rotating Vortex Formations.

it is obvious the destabilizing effect the spoilers have on the tip vortex. From these figures, it is seen that increasing the spoiler size has the effect of “unwinding” the tip vortex. This “unwinding” or diffusion of the tip vortex is what is desired in order to improve the BVI characteristics of the blade.

Finally, the computed thrust and torque coefficients for the two largest spoilers are  $C_T = 0.0044$  and  $C_Q = 0.00058$  (spoiler #2), and  $C_T = 0.0040$  and  $C_Q = 0.00119$  (spoiler #3). As expected, the trends show that the thrust decreases and the torque increases as the spoiler size increases when compared with the values calculated for the clean rotor.

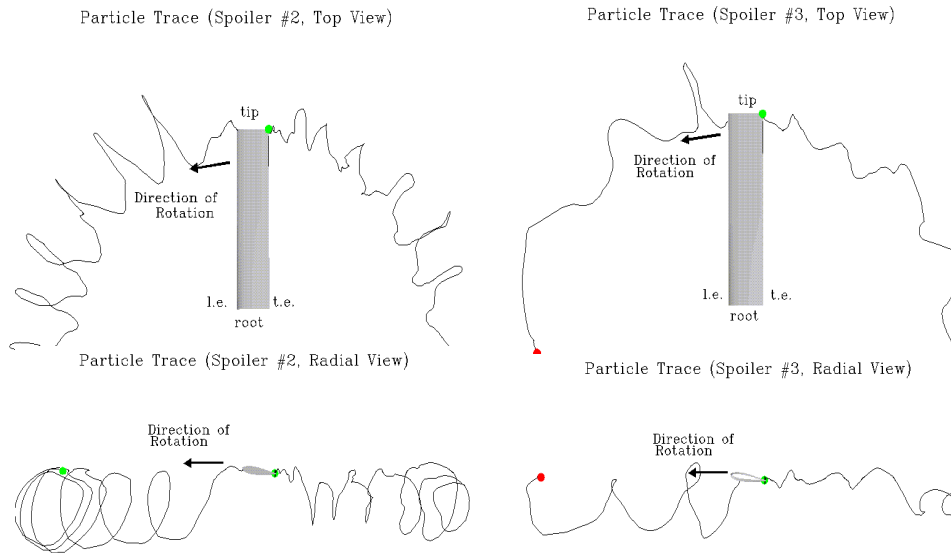


**Figure 14:** Particle Traces Around the Azimuth for the Rotor with Various Trailing-Edge Spoilers

## 6. Conclusions

A high-order spatial accuracy scheme is capable of capturing the rotor tip vortex over large distances, provided enough grid points remain distributed through the vortex core. However, many revolutions are potentially needed to allow the rotor wake to develop and to accurately capture the rotor tip vortex with respect to all three coordinate velocity distributions (especially the inboard direction), as well as to yield accurate performance predictions.

It has been shown that reasonable qualitative and quantitative results about the vortex core in the normal and axial directions can be captured within one half of a rotor revolution. This can lead to less computational effort if only general effects on the vortex due to some rotor modification (i.e., implementation of a passive tip device) are desired. With this in mind, a trailing edge spoiler has been shown to yield a beneficial effect with regards to destabilization and/or diffusion of the rotor tip vortex in hover, which leads to better BVI characteristics for the blade. The larger the spoiler, the more the diffusion/destabilization there is to the tip vortex.

Further studies are needed to determine an “ideal” spoiler for a given rotor configuration and flight condition (i.e., the spoiler yielding the most destabilizing effects for the least amount of performance penalty), both in terms of spoiler size and location. Finally, convergence to a steady state is necessary to yield accurate performance predictions for both the clean rotor and the trailing-edge spoiler configurations.

## Acknowledgements

The first two authors acknowledge the support of the National Rotorcraft Technology Center (NRTC) for this project, as part of the Georgia Tech Rotorcraft Center of Excellence.

## References

- Lee, D.J. and Smith, C.A., “Effect of Core Distortion on Blade-Vortex Interaction,” *AIAA Journal*, Vol. 29, (9), September 1991.
- Tangler, J.L., “Experimental Investigation of the Subwing Tip and Its Vortex Structure,” NASA CR 3058, 1978.
- Berry, J.D., and Mineck, R.E., “Wind Tunnel Test of An Articulated Helicopter Rotor Model with Several Tip Shapes,” NASA TM 80080, December 1980.
- Smith, D.E. and Sigl, D., “Helicopter Rotor Tip Shapes for Reduced Blade Vortex Interaction An Experimental Investigation,” AIAA Paper 95-0192.
- Wake, B.E., and Choi, D., “Investigation of high-order upwinded differencing for vortex convection,” *AIAA Journal*, Vol. 34, February 1996.
- Yu, Y.H., “Rotor Blade-Vortex Interaction Noise: Generating Mechanisms and its Control Concepts,” American Helicopter Northeast Region Aeromechanics Specialist Meeting, Bridgeport, CT, October 1995.
- McAlister, K.W., Schuler, C.A., Branum, L., and Wu, J.C., “3-D Wake Measurements Near a Hovering Rotor for Determining Profile and Induced Drag,” NASA Technical Paper 3577, August 1995.
- Leibovich, S. and Stewartson, K., “A sufficient condition for the stability of columnar vortices,” *Journal of Fluid Mechanics*, Vol. 126, July 1982.

- Stewartson, K. and Leibovich, S., "On the stability of a columnar vortex to disturbances with large azimuthal wavenumber: the lower neutral points," *Journal of Fluid Mechanics*, Vol. 178, August 1986.
- Russell, J.W., Sankar, L.N., Tung, C., and Patterson, M.T., "Alterations of the Tip Vortex Structure from a Hovering Rotor using Passive Tip Devices," American Helicopter Society 53<sup>rd</sup> Annual Forum, Virginia Beach, Virginia, April 29 - May 1, 1997.
- Hariharan, N., "High Order Simulation of Unsteady Compressible Flows Over Interacting Bodies with Overset Grids," Ph.D. Thesis, Georgia Institute of Technology, Atlanta, GA, August 1995.
- Roe, P.L., "Approximate Riemann Solvers, Parametric Vectors, and Difference Schemes," *Journal of Computational Physics*, Vol. 39, 1981.
- Chakravarthy, C.R., "Some Aspects of Essentially Nonoscillatory (ENO) Formulations for the Euler Equations," NASA CR 4285, May 1990.
- Harten, A. and Chakravarthy, C.R., "Multi-Dimensional ENO Schemes for General Geometries," NASA CR 187637, September 1991.
- Pulliam, T. H. and Chaussee, D.S., "A Diagonal Form of an Implicit Approximation -Factorization Algorithm," *Journal of Computational Physics*, Vol. 39, 1981.
- Russell, J.W., Sankar, L.N., and Tung, C., "High Accuracy Studies of the Tip Vortex Structure from a Hovering Rotor," AIAA Paper 97-1845